Multidisciplinary Research Journal
ISSN (online): 3108 – 1533

Volume 2, Issue 1, 2026
January – March 2026

Research Article

Response of Hydrogeochemical Variables and Heavy Metals to Flooding in Surface Water of Jia Bharali River, India

Jigyashree Lahon [1], Rocktim Baruah [1], Sumi Handique [1,*]

[1] Department of Environmental Science, Tezpur University, Assam, INDIA-784028
* Correspondence: sumihan@tezu.ernet.in

Scopus Author ID: 57191596223

Received: 26 September 2025; Accepted: 30 March 2026; Published: 29 April 2026

Abstract: As compared to groundwater, surface water bodies are more prone to degradation due to their direct exposure to environmental contaminants. The present study aims to conduct an in-depth hydrogeochemical evaluation of surface water of Jia Bharali River, a significant tributary of Brahmaputra River in northeastern India, in response to flooding. Twelve sampling sites were selected along the entire river stretch within the Assam plain during pre-flood and post-flood periods of 2024 and they were analysed for 21 physicochemical parameters, including major cations, anions, and heavy metals. Various pollution indices employed for heavy metals showed low level of pollution for both pre-flood and post-flood seasons. Multivariate statistical methods were employed to identify water quality similarities and dissimilarities across sites and their possible sources of contamination. The total hardness (TH) content was found to be high across the sampling sites during both seasons. The trilinear piper plot diagram indicated that the river water is dominated by Ca^{2+}-Mg^{2+}-HCO_3^- type. The Gibbs plot further revealed that hydrogeochemistry is primarily governed by rock-water interaction. The overall water quality of Jia Bharali River is appropriate for its usage during both seasons; however, proper monitoring and management measures need to be adopted to ensure sustainable and safe use of the Jia Bharali River, especially after flood events. It will help to mitigate the potential risks of pollutants to human health and the overall river ecosystem posed by floodwater.

Keywords: Hydrogeochemistry; Flooding; Surface water; Heavy metal; Pollution indices

1. Introduction

Rivers are fundamental to the development of human societies and support countless ecosystems [1]. However, pollution-related activities have drastically altered the aquatic environment over the past several decades [2]. Elevated pollutant levels in natural water systems are a significant concern due to their potential risks to both human health and ecosystems [3]. The physicochemical characteristics of freshwater resources in Himalayan ranges as well as the Western Ghats are adversely affected due to flooding, landslides, and earthquakes [4]. Flood hazards in river catchment areas lead to mixing of pollutants from various sources, which alters geochemical processes, ion exchange processes that ultimately impacts the availability of freshwater [4,5]. Characteristics of catchment like geology, climate, terrain, land uses, and anthropogenic activities, significantly alter the spatiotemporal distribution of river water chemistry [6]. The river water quality is primarily affected by biogeochemical and hydrogeological processes, as well as the interlinkage between humans and the environment, leading to deterioration of water resources [7].

During monsoon season, the Brahmaputra River along with its tributaries causes flooding in Assam plains [8]. The lower section of Jia Bharali River, part of the river where it enters Assam, is prone to frequent flooding [9]. During monsoon period, excessive rainfall occurs, which results in flooding of the nearby adjacent areas of the river as the excess water transcends the river's capacity to hold it, thus severely impacting the settlements nearby [10]. Being one of the largest tributaries of Brahmaputra, it has undergone considerable transformation over time due to urban expansion, increased agricultural activities, and industrial development. These changes have resulted in a rise in pollution levels, especially in surface water. Previous studies indicate that iron concentrations in certain areas exceed the recommended levels, raising concerns about possible health implications [11].

Existing studies to observeing the impact of flood hazard on the hydrogeochemical parameters in various environmental compartments were conducted in groundwater [4,12], river sediments [13], and lakes [12]. However, very few studies have investigated the flooding impact on the hydrogeochemistry of rivers in Northeast India. As a result, there exists a research gap in understanding the response of hydrogeochemical variables, especially during pre-flood and immediately after flooding periods, and to examine specific natural or anthropogenic sources of pollutants. For a comprehensive water quality evaluation, the assessment of only heavy metals or a limited range of physicochemical parameters is not sufficient, as they cannot represent the full spectrum of potential contaminants in a river and thus may hinder the development of effective pollution control strategies. Thus, the present study aims to narrow the research gap by investigating the variation of hydrogeochemical parameters and their levels of contamination before and after the flood event in a river.

2. Materials and Methods

2.1 Study Site

The Jia Bharali River, which flows through the centre of Tezpur city of Assam, is one of the significant tributaries of the river Brahmaputra [14]. It originates from a glacial lake in the hills of Arunachal Pradesh. The main channel that precedes the Jia Bharali, known as the Kameng River (in Arunachal Pradesh), crosses the Himalayan thrust and it emerges into the plains at Bhalukpung (92º65′E,27º01′N) [15]. Out of the total catchment area of the river, only 929 sq.km lies in Assam, and the remaining 9360 sq.km lies in Arunachal Pradesh [16]. In the present study, the entire river stretch of Jia Bharali was selected that lies in the Assam plain, starting from Bhalukpung to the confluence point near the Kolia Bhomora Bridge situated at Tezpur (Figure1). The sampling sites along with their respective coordinates and elevations are shown in Appendix, Table S1. This stretch of the river is highly flood-prone and thus aligns with the goals of our study. Agricultural fields, mainly rice paddies, mustard crops, and tea gardens, are located in adjacent areas of the river stretch due to its rich alluvial deposits.

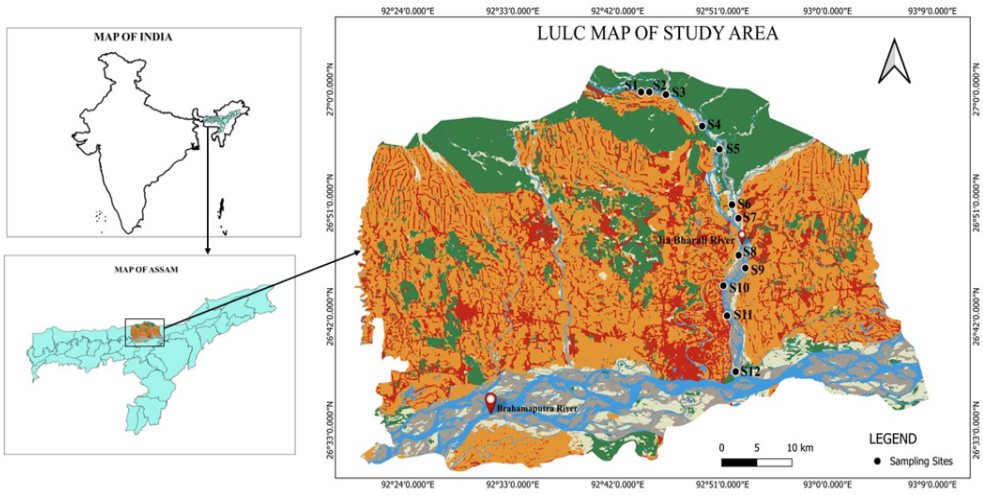

Figure 1. Study area map showing the sampling sites along the stretch of Jia Bharali River. during both pre-flood and post-flood periods 2024

2.2. Sample Collection and Storage

We selected 12 different locations along the Jia-Bharali River for the collection of surface water samples before (April) and after (August) the flood event of 2024. Triplicate water samples were collected from each location using pre-cleaned 2-liter polypropylene bottles. Before sample collection, bottles were thoroughly rinsed with deionised water and washed properly. Immediately after collection, nitric acid was added to the samples for heavy metal analysis [17]. For the analysis of the remaining physicochemical parameters, samples were preserved at 4°C until analysis [18].

2.3. Analysis of Physicochemical Parameters

On-site measurement of pH, EC and DO were carried out using digital multiparameter waterproof meter (HANNA, HI98194). Total Dissolved Solids (TDS) was also measured using the multiparameter probe. Standard methods of APHA (American Public Health Association) [19] were followed in the collection, and analysis of the water samples. Major cations (Na^+, K^+, Ca^{2+}, and Mg^{2+}) were determined using ICP-OES (Inductively Coupled Plasma Optical Emission Spectroscopy) (Perkin Elmer, AVIO 220 MAX) after appropriate sample digestion and filtration. All the heavy metals were also analysed using ICP-OES. Sulphate (SO_4^{2-}) concentration was measured using UV-Visible spectrophotometer (UV-2600i). For chloride (Cl^-),. bicarbonate (HCO_3^-) and total hardness (TH) estimation of the water samples the methods of APHA were followed [19].

2.4. Heavy Metal Contamination Indices

Heavy Metal Pollution Index (HPI)

The combined effect of various heavy metals on the overall water quality is reflected by HPI [20]. It is determined through a weighted arithmetic mean approach, which takes into account the concentration of each metal, its corresponding permissible limit and weight assigned to it by WHO (2017) [21].

The HPI model was given by [22] shown in Eqs (1-3)

Sub- index (Qi):

$$Q_i = \left(\frac{M_i}{S_i}\right) \times 100 \quad (1)$$

Unit weight (Wi):

$$W_i = \frac{K}{S_i} \quad (2)$$

HPI calculation:

$$\frac{\sum_{i=1}^{n} Q_i W_i}{\sum_{i=1}^{n} W_i} \quad (3)$$

where:
M_i is the measured concentration of the i^{th} metal (mg/L),
S_i is the standard permissible value for the i^{th} metal (mg/L),
W_i is the unit weight assigned to the i^{th} metal,
Q_i is the sub index of the i^{th} metal,
N is the number of the metals considered.

An HPI value less than 100 indicates low pollution, whereas if the values exceeding 100 suggest significant heavy metal contamination.

Heavy Metal Evaluation Index (HEI)

The overall assessment of the water quality in relation to its heavy metal content is given by HEI as shown in Eq (4) [23]

$$HEI = \sum_{i=1}^{n} \frac{H_c}{H_{MAC}} \quad (4)$$

where:
H_c is the measured concentration of the i^{th} metal (mg/L),
H_{MAC} is the maximum admissible concentration for the i^{th} metal (mg/L),
n is the number of the metals analyzed.

The HEI categorizes water quality into three levels: Low (HEI < 10), medium (10 < HEI < 20) and highly polluted (HEI > 20)

Contamination Index (C_d)

The level of contamination that is harmful for various domestic applications is shown by C_d. It is the summation of all contaminant factors shown in Eq (5) [23].

$$C_d = \sum_{i=1}^{n} C_{fi} \quad (5)$$

where:
C_{fi} is the ratio between the concentration of each metal C_{metal} to the background values $C_{background}$, shown in Eq (6) [24]

$$C_{fi} = \frac{C_{metal}}{C_{background}} \quad (6)$$

The C_d classifies the water as low, medium and high for $C_d < 1$, C_d = 1-3, and $C_d > 3$, respectively [23].

Pollution Load Index (PLI)

PLI is calculated to measure the entire heavy metal concentration in a site by taking into consideration multiple heavy metal values into a single index value, thereby indicating the cumulative pollution status of the sampling sites shown in Eq (7) [25].

$$PLI = (CF_1 \times CF_2 \times CF_3 \times \ldots\ldots \times CF_n)^{1/n} \quad (7)$$

where:
CF_n = contamination Factor for the n^{th} metal may be expressed as Eq (8)

$$CF_n = \frac{C_n}{B_n} \quad (8)$$

where:
C_n = concentration of the heavy metal
B_n = background or reference value of the metal
If PLI < 1, it means no metal pollution exists, and if PLI > 1, it means pollution exists [25].

The reference/background values used in the calculation of C_d and PLI in the present study are the acceptable limits of the heavy metals prescribed by Bureau of Indian Standard (BIS) drinking water specifications [26]. As our study area lies in the Indian subcontinent so the Indian standard values were considered. This approach was also adopted in a previous study conducted in the Indian subcontinent [27].

2.5. Statistical Analysis

To observe the significance of variation of physicochemical parameters between different sampling sites one-way analysis of variance (ANOVA) was performed. Paired t-test was carried out to find whether there was any significant difference between pre-flood and post-flood seasons. Piper plot and Gibbs plot diagrams to find the major hydrochemical facies and the dominant factor controlling surface water chemistry, respectively, were created using Origin Pro software. Principal Component Analysis (PCA) and Hierarchical Cluster Analysis (HCA) were employed using Origin Pro.

2.6. Quality Assurance and Quality Control

The study employed strict and standardized protocols to guarantee quality and reliability of the data collected. Instruments used for the measurement of water samples for various physicochemical parameters were calibrated on a regular time interval. Analytical

blanks and triplicates were analyzed to monitor precision and accuracy in every step. All glassware were rinsed properly with de-ionized water to get rid of laboratory contamination. The reagents were freshly prepared in accordance with the requirements. A blank sample was used to measure specificity for those chemical parameters of water analyzed by using ICP-OES.

3. Results and Discussion

The values of the physicochemical parameters of Jia Bharali River are shown in Table 1 and 2 for both the seasons. The shifting of pH to a more alkaline range during post-flood, compared to pre-flood, is likely due to intensified contact between rainwater and surrounding soils/rocks during monsoon, enhancing the dissolution of alkaline minerals into the river system [28]. Electrical conductivity (EC) dropped during the post-flood period, which might result from the influx of various ions introduced through point and non-point sources [29]. The low DO concentration during the pre-flooding period may be linked to the lower water volume, whereas the elevated DO concentrations during the monsoon can be attributed to increased water flow resulting from heavy rainfall [30]. An increase in the total dissolved solids (TDS) was recorded during post-flood compared to pre-flood period. This increase may be due to runoff water during the flooding period, which carries organic matter and sediments into the river, increasing the TDS. High total hardness during pre-flooding season might be due to reduced water levels and high rate of evaporation and decomposition, leading to a the high concentration of dissolved salts in the water samples. COD of the water samples increases during post-flooding period compared to pre-flooding period. This might be attributed to the introduction of organic matter and contaminants from the surrounding area through runoff during flooding period. A slight change in biological oxygen demand (BOD) was observed between both the seasons. Most of the physicochemical parameters fall within the acceptable limits as recommended by WHO [31]. EC, DO, TDS and TH values fall within acceptable limits prescribed by WHO [31] and BIS [26]. The pH value of pre-flood shifted to a more alkaline range during post-flood period. BOD of all the water samples and COD of all the water samples, except site S1 of the post-flooding season showed concentration above the standard limit (30 mg/l for BOD and 250 mg/l for COD) as per the Environment (Protection) Rules, 1986 [32]. Site S1 is located at the border of Assam and Arunachal Pradesh which receives various pollutants from sources like agricultural runoff, sewage and domestic discharge. Increased COD level can lead to disruption of the aquatic ecosystem, degrade water quality and reduce aquatic biodiversity In Ramganga River of India, an increase in BOD during the dry season and a decline in monsoon period were observed due to dilution of anthropogenic sources [33]. However, their study did not account for the impact of floods on hydrogeochemical parameters. ANOVA results showed no significant differences ($p>0.05$) across sites for most of the parameters (pH, EC, alkalinity, BOD, COD, TDS), except for DO ($p = 0.012$), indicating significant spatial variation in oxygen levels. Paired t-test revealed significant difference between the two seasons for physicochemical parameters ($p = 0.006$), suggesting seasonal influences on river water.

Table 1. Descriptive statistics of water quality parameters of Jia Bharali River during pre-flooding period of 2024

Sites	pH	EC	DO	TH	BOD	COD	TDS	Na^+	K^+	Ca^{2+}	Mg^{2+}	HCO_3^-	SO_4^{2-}	Cl^-
S1	6.78 ± 0.03	179 ± 0.02	7.6 ± 0.04	130 ± 0.05	2.9 ± 0.06	190 ± 0.03	130 ± 0.007	10.22 ± 78.6	3.805 ± 42.35	12.27 ± 76.06	3.392 ± 33.84	83 ± 0.27	17.313 ± 0.078	74.55 ± 0.95
S2	6.47 ± 0.03	160 ± 0.04	7.1 ± 0.05	125 ± 0.14	2.6 ± 0.01	160 ± 0.01	98 ± 0.006	3.121 ± 40.26	2.083 ± 21.94	15.55 ± 58.65	42.6 ± 0.22	63 ± 0.17	11.162 ± 0.06	42.6 ± 0.22
S3	6.81 ± 0.04	151 ± 0.10	7.8 ± 0.05	92 ± 0.01	2.4 ± 0.04	113 ± 0.08	127 ± 0.66	3.542 ± 41.68	2.033 ± 12.11	14.72 ± 46.07	49.7 ± 0.04	86 ± 0.07	17.58 ± 0.12	49.7 ± 0.04
S4	7.51 ± 0.04	178 ± 0.07	7.7 ± 0.32	80 ± 0.17	3.8 ± 0.02	143 ± 0.5	125 ± 0.62	11.27 ± 47.48	3.733 ± 22.74	11.73 ± 47.06	3.352 ± 27.07	66 ± 0.01	28.915 ± 0.02	60.35 ± 0.08
S5	7.5 ± 0.05	158 ± 0.01	7.9 ± 0.02	275 ± 0.10	3.6 ± 0.01	130 ± 0.09	129 ± 0.11	10.1 ± 46.87	3.139 ± 11.67	10.05 ± 42.32	56.8 ± 0.01	86 ± 0.01	16.805 ± 0.08	56.8 ± 0.01
S6	7.52 ± 0.04	138 ± 0.02	7.2 ± 0.01	160 ± 0.01	2.4 ± 0.15	108 ± 0.08	114 ± 0.004	7.864 ± 44.07	2.536 ± 54.39	9.172 ± 16.44	2.486 ± 30.84	66 ± 0.27	25.942 ± 0.05	74.55 ± 0.01
S7	7.43 ± 0.03	158 ± 0.26	8 ± 0.01	82.5 ± 0.28	3.8 ± 0.11	94 ± 0.02	110 ± 0.17	9.367 ± 76.57	3.037 ± 29.58	10.56 ± 23.12	49.7 ± 0.06	66 ± 0.13	18.071 ± 0.08	49.7 ± 0.06
S8	7.59 ± 0.04	118 ± 0.28	6.6 ± 0.20	160 ± 0.07	2.8 ± 0.08	100 ± 0.04	90 ± 0.023	8.97 ± 46.27	2.849 ± 23.31	9.636 ± 57.93	56.8 ± 0.32	43 ± 0.01	22.821 ± 0.11	56.8 ± 0.32
S9	7.34 ± 0.04	170 ± 0.02	6.2 ± 0.03	140 ± 0.24	2.2 ± 0.05	113 ± 0.01	118 ± 0.28	7.743 ± 27.17	3.569 ± 10.03	14.21 ± 72.46	3.456 ± 13.33	70 ± 0.04	19.022 ± 0.07	39.05 ± 0.01
S10	6.98 ± 0.02	172 ± 0.01	7 ± 0.01	117.5 ± 0.02	2.5 ± 0.05	109 ± 0.19	120 ± 0.109	9.772 ± 33.90	3.665 ± 5.96	12.83 ± 30.55	3.39 ± 17.34	76 ± 0.06	14.343 ± 0.05	53.25 ± 0.01
S11	6.84 ± 0.02	135 ± 0.07	6.9 ± 0.01	165 ± 0.07	2.1 ± 0.06	64 ± 0.6	105 ± 0.11	5.611 ± 9.65	2.098 ± 34.39	10.39 ± 38.43	2.472 ± 15.22	60 ± 0.02	24.429 ± 0.03	46.15 ± 0.01
S12	6.81 ± 0.02	120 ± 0.01	6.1 ± 0.26	80 ± 0.01	2.3 ± 0.01	97 ± 0.50	95 ± 0.83	5.331 ± 35.25	2.066 ± 2.60	10.69 ± 33.23	2.53 ± 8.71	60 ± 0.18	14.383 ± 0.03	46.15 ± 0.07
Max	7.59	179	8	275	3.8	190	130	11.27	3.81	15.55	3.46	86	28.92	74.55
Min	6.47	118	6.1	80	2.1	64	90	3.12	2.03	9.17	2.47	43	11.16	39.05
Range	1.12	61	1.9	195	1.7	126	40	8.15	1.77	6.38	0.98	43	17.75	35.50

Unit of 'EC' is µS/cm, and for other parameters, except pH, is mg/L

Table 2. Descriptive statistics of water quality parameters of Jia Bharali River during post-flooding period of 2024

Sites	pH	EC	DO	TH	BOD	COD	TDS	Na^+	K^+	Ca^{2+}	Mg^{2+}	HCO_3^-	SO_4^{2-}	Cl^-
S1	7.8 ± 0.2	90 ± 2	8.2 ± 0.2	220 ± 0.012	2.6 ± 0.2	300 ± 0.09	220 ± 0.17	0.442 ± 0.001	0.1617 ± 0.00004	0.872 ± 0.007	0.216 ± 0.002	206 ± 1	12.307 ± 0.01	56.8 ± 2.0
S2	7.6 ± 0.3	94 ± 1.0	8 ± 0.1	200 ± 0.47	1.3 ± 0.2	100 ± 0.22	140 ± 0.17	0.1831 ± 0.002	0.08823 ± 0.002	0.556 ± 0.009	0.129 ± 0.002	116 ± 1.7	23.04327± 0.14	42.6 ± 0.1
S3	8.1 ± 0.2	92 ± 2.0	7.9 ± 0.1	156 ± 0.13	2.7 ± 0.1	200 ± 0.36	126 ± 0.10	0.3109 ± 0.001	0.1398 ± 0.001	0.876 ± 0.004	0.216 ± 0.002	106 ± 1	18.4565 ± 0.15	36.92 ± 0.01
S4	7.8 ± 0.2	120 ± 1.7	8 ± 0.5	164 ± 0.22	3.1 ± 0.3	165 ± 0.10	160 ± 0.07	0.2098 ± 0.002	0.1209 ± 0.001	1.06 ± 0.007	0.225 ± 0.001	136 ± 0.5	22.3842 ± 0.28	28.4 ± 0.02
S5	8.8 ± 0.1	110 ± 1.7	7.6 ± 0.2	140 ± 0.48	2.4 ± 0.3	180 ± 0.30	271 ± 0.30	0.1393 ± 0.001	0.1093 ± 0.001	1.191 ± 0.006	0.227 ± 0.001	250 ± 0.8	19.3329 ± 0.21	36.92 ± 0.01
S6	7.8 ± 0.2	104 ± 2.5	7.8 ± 0.1	196 ± 0.19	2.6 ± 0.1	210 ± 0.13	298 ± 0.10	0.1248 ± 0.002	0.09574 ± 0.002	1.154 ± 0.004	0.218 ± 0.002	280 ± 1	16.40746± 0.20	36.92 ± 0.01
S7	7.8 ± 0.1	102 ± 2.0	8.2 ± 0.1	140 ± 0.05	2.6 ± 0.2	75 ± 0.09	210 ± 0.20	0.1258 ± 0.001	0.1226 ± 0.001	1.219 ± 0.003	0.216 ± 0.001	190 ± 1.6	18.2644 ± 0.12	17.04 ± 0.01
S8	7.7 ± 0.2	96 ± 2.1	7.1 ± 0.2	164 ± 0.13	2.3 ± 0.1	115 ± 0.13	186 ± 0.10	0.2708 ± 0.0007	0.1403 ± 0.001	1.053 ± 0.015	0.208 ± 0.002	163 ± 1	21.295 ± 0.17	34.08 ± 0.01
S9	7.6 ± 0.1	105 ± 1.5	6.8 ± 0.1	188 ± 0.11	2.3 ± 0.1	78 ±0.17	139 ± 0.17	0.2587 ± 0.004	0.1328 ± 0.002	1.12 ± 0.004	0.218 ± 0.002	120 ± 1	17.2472 ± 0.13	14.2 ± 0.1
S10	7.8 ± 0.1	108 ± 2.0	7.5 ± 0.2	152 ± 0.22	2.2 ± 0.2	89 ± 0.10	185 ± 0.13	0.1223 ± 0.001	0.1256 ± 0.0002	1.313 ± 0.006	0.216 ± 0.002	160 ± 3	23.2169 ± 0.20	19.88 ± 0.10
S11	8 ± 0.3	96 ± 1.0	7.6 ± 0.3	192 ± 0.03	2.6 ± 0.1	120 ± 0.15	170 ± 0.22	0.298 ± 0.018	0.185 ± 0.015	0.636 ± 0.008	0.221 ± 0.11	140 ± 0.5	28.66 ± 0.21	31.24 ± 0.04
S12	7.7 ± 0.2	122 ± 1.7	6.8 ± 0.1	124 ± 0.27	2.7 ± 0.2	107 ± 0.17	175 ± 0.10	0.312 ± 0.012	0.162 ± 0.01	1.098 ± 0.036	0.284 ± 0.02	150 ± 0.7	23.044 ± 0.13	14.2 ± 0.1
Max	8.1	122	8.2	220	3.1	300	298	0.44	0.26	1.31	0.28	280	28.66	56.80
Min	7.6	90	6.8	124	1.3	75	126	0.12	0.09	0.56	0.13	106	12.31	14.20
Range	0.5	32	1.4	96	1.8	225	172	0.32	0.17	0.76	0.15	174	16.35	42.60

Unit of 'EC' is µS/cm, and for other parameters, except pH, is mg/L

3.1. Hydrogeochemical Characterization of Major Ions

The major ion concentration of the water samples during pre & post-flooding periods are shown in Table 1 and 2, respectively. It reveals seasonal variation, significantly higher values during pre-flooding compared to post-flooding season. The ionic dominance pattern follows the order $Ca^{2+} > Na^+ > Mg^{2+} > K^+$ for cations , and $HCO_3^- > Cl^- > SO_4^{2-}$ anions during both pre & post-flood season. High bicarbonate content mainly comes from the carbonate and bicarbonate rocks of calcium and magnesium. A study reported similar findings in the study on Chaliyar River, Kerala [30]. Chloride and sulphate ions in the river water made their way through agricultural runoff and atmospheric deposition along with lithological formations like halites and sulphide-bearing rocks. The major sources of Ca^{2+} and Na^+ are the weathering of Ca^{2+} and Na^+ bearing minerals such as pyroxene. The presence of Mg^{2+} may be due to the weathering of dolomite rock, followed by K^+. Similar results were also reported in a previous study [34]. Thus, the overall hydrogeochemical composition of the river indicates a strong

influence of natural geological weathering and seasonal change in hydrology, with geogenic factors.

The trilinear piper plot diagram (Figure 2) revealed that, for both the seasons, the river water is dominated by Ca^{2+} -Mg^{2+} -HCO_3^- type. In Koyna River basin, similar results were obtained for the majority of the water samples [35]. In another study conducted at Parbati River, Northwestern Himalaya, where the piper diagram indicated that both the pre & post-flood samples were dominated by Ca^{2+}- Mg^{2+} -HCO_3^- type [36]. The regional geological features, rock water interactions, chemical weathering and relative mobility of ions plays a crucial role in determining the ionic composition of natural water [37,38]. The Gibbs plot diagram (Figure 3) revealed that all the water samples from both seasons fall within rock-dominance region which means rock weathering processes dominate the chemical composition of the water samples of Jia Bharali River rather than atmospheric precipitation and evaporation. Both the cationic and anionic plot of the Gibbs diagram revealed that the chemical composition of river water during pre & post-flood seasons is primarily controlled by interactions between water and geological materials.

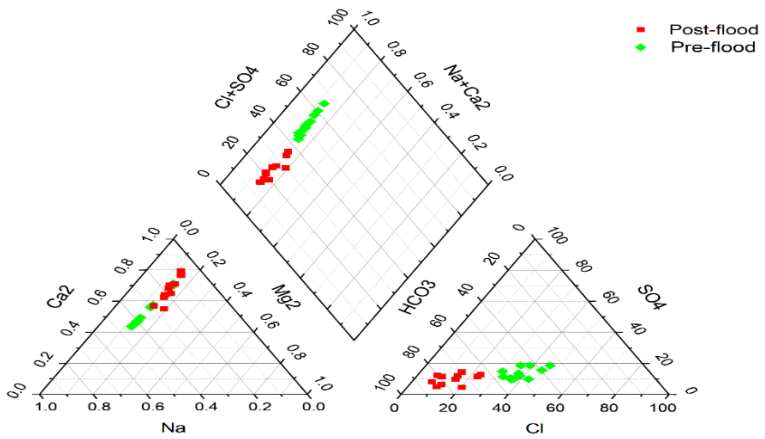

Figure 2. Piper plot diagram of surface water samples of Jia Bharali River during pre-flood and post-flood periods 2024

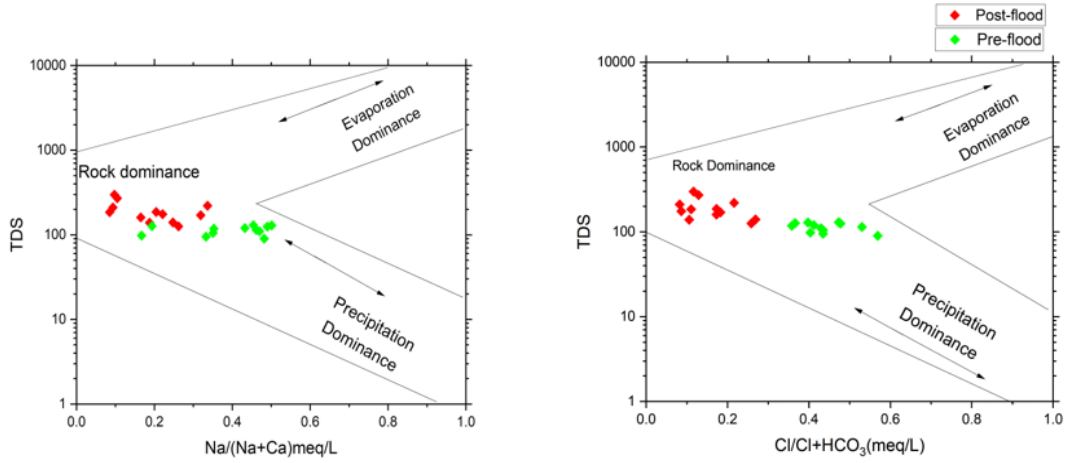

Figure 3. Gibbs plot diagram of surface water samples of Jia Bharali River during pre-flood and post-flood periods, 2024

3.2. Heavy Metal Contamination Indices

Heavy metal contamination in the Jia Bharali River during both seasons was evaluated using various pollution indices: HPI, HEI, C_d, and PLI (Table 3). During pre-flooding season,

HPI values ranged from 0.014 to 8.742, which is below the critical limit of 100, with the highest pollution observed at site 2, i.e 8.742. HEI values also remained below the threshold value (HEI < 10), which indicate low pollution (maximum 0.0743 at site 1). C_d values ranged from 0.074 to 0.503, indicating values less than the critical limit of < 1, though relatively elevated at sites 1, 2, and 8. PLI ranges from 0.0009 to 0.0266, which is far below the threshold (PLI > 1), indicating the absence of pollution. In the post-flooding season, all indices showed further reductions, which may be attributed to dilution from monsoonal rainfall and floodwater. The HPI ranged from 0.035 to 2.002 (highest at site 7), HEI values remained below 0.065, C_d ranged from 0.013 to 0.467, and PLI ranged from 0.0006 to 0.0177, which indicating that heavy metal concentrations are within safe limits. However, the pre-flooding season had slightly elevated values compared to post-flooding, suggesting regular monitoring, especially during periods of low flow and higher anthropogenic activity. The heavy metal concentration at each sampling location of Jia Bharali River during both the seasons is shown in Appendix, Table S2 and S3, respectively. The concentrations of Ni and Cd were found to be below the detection limit during pre-flooding and post-flooding periods, respectively. The rainfall data for the two sampling seasons are presented in Table S4 (*Appendix*).

Table 3. Heavy metal indices and their contamination level at all the sampling locations of Jia Bharali River

Sites	**Pre-flood**								**Post-Flood**							
	HPI	**Level**	**HEI**	**Level**	**C_d**	**Level**	**PLI**	**Category**	**HPI**	**Level**	**HEI**	**Level**	**C_d**	**Level**	**PLI**	**Category**
S1	4.470	Low	0.074	Low	0.502	Low	0.026	No pollution	0.073	Low	0.007	Low	0.051	Low	0.003	No pollution
S2	8.742	Low	0.043	Low	0.296	Low	0.004	No pollution	0.421	Low	0.024	Low	0.168	Low	0.004	No pollution
S3	2.685	Low	0.023	Low	0.160	Low	0.001	No pollution	1.865	Low	0.016	Low	0.112	Low	0.006	No pollution
S4	0.767	Low	0.013	Low	0.089	Low	0.001	No pollution	0.187	Low	0.011	Low	0.072	Low	0.002	No pollution
S5	1.071	Low	0.043	Low	0.293	Low	0.006	No pollution	0.121	Low	0.006	Low	0.045	Low	0.002	No pollution
S6	0.028	Low	0.026	Low	0.180	Low	0.001	No pollution	0.076	Low	0.003	Low	0.056	Low	0.002	No pollution
S7	3.264	Low	0.047	Low	0.318	Low	0.001	No pollution	2.002	Low	0.064	Low	0.467	Low	0.006	No pollution
S8	4.603	Low	0.048	Low	0.327	Low	0.001	No pollution	0.541	Low	0.030	Low	0.205	Low	0.003	No pollution
S9	1.142	Low	0.011	Low	0.074	Low	0.002	No pollution	0.220	Low	0.013	Low	0.087	Low	0.002	No pollution
S10	1.567	Low	0.024	Low	0.163	Low	0.006	No pollution	0.035	Low	0.002	Low	0.013	Low	0.001	No pollution
S11	1.765	Low	0.030	Low	0.202	Low	0.005	No pollution	1.130	Low	0.019	Low	0.130	Low	0.007	No pollution
S12	0.014	Low	0.011	Low	0.076	Low	0.026	No pollution	1.965	Low	0.034	Low	0.282	Low	0.017	No pollution

3.3. Hierarchical Cluster Analysis

HCA was performed to identify clusters of river sampling sites according to their water quality similarities by applying Ward's method for both pre- and post-flood periods. The clusters or groups that are produced through this technique have high internal homogeneity but high external heterogeneity [19]. The HCA conducted for pre-flooding season for the sampling sites generated three distinct clusters (Figure 4) having similar characteristics and same source of contamination. Cluster 1 consisted of sampling sites S1 and S5, which are located in the upstream of the river. The pollutants at these two sites may be attributed to the various tourism activities in the river and nearby agricultural fields. Cluster 2 consisted of the majority of the sampling sites of the river S2, S3, S4, S8, S9, S10, S11 and S12. This cluster included sites situated in all upstream, midstream and downstream of the river, The primary cause of contamination in these regions may be due to various anthropogenic and hydrological factors. Cluster 3 consisted of sites S6 and S7, located in the midstream of the river.Anthropogenic inputs like discharge from nearby rural households, farmlands and cattle farms are the potential sources that lead to the contamination at site S7. The HCA conducted for post-flooding season for the sampling locations of the river produced five clusters. Cluster 1 consisted of sites S1 and S12, located upstream and downstream of the river, respectively. The contaminants at these two sites may come from fishing gears, antifouling paints and fuel/oil leakage from boats, and other recreational activities along the bank of the river. Sampling site S12 is relatively highly polluted, as it is the confluence point of Jia Bharali. River confluence is the area of highest concentration of pollutants, initially forming a highly polluted region which is compressed and gets dispersed later on [39]. Cluster 2 consisted of sites S2, S4, S5, S6, S9, S10 and S11, which may be associated with anthropogenic activities like farming and fishing activities. Clusters 3, 4 and 5 consisted of sites S3, S8 and S7, respectively. The variation in the pollution level in locations S3, S6, S7, S11 and S12 during pre-flood to post-flood periods may be attributed to geogenic factors and dilution of river water during the flood period.

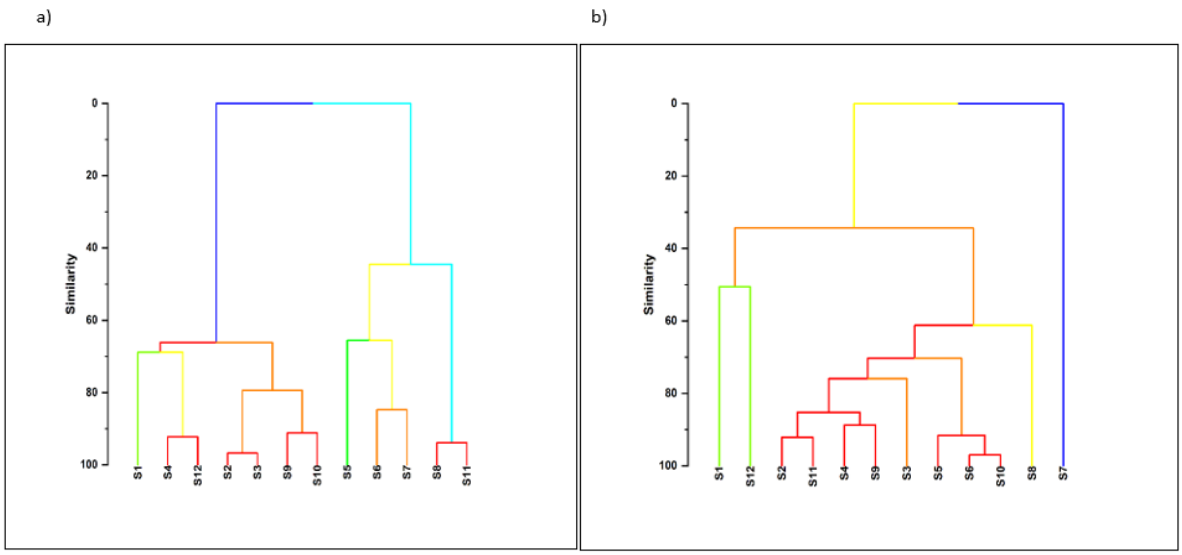

Figure 4. Dendrogram based on hierarchical clustering for all the sampling locations of Jia Bharali River during a) pre-flood, and b) post-flood periods, 2024

3.4. Principal Component Analysis

The PCA biplot for river water quality parameters during pre-flood and post-flood periods reveal distinct seasonal patterns in the distribution and influence of various physicochemical parameters. Varimax rotation method was used to extract the principal components (PCs). Two major PCs were extracted (Figure 5) during both the seasons, which capture most variance in the data. During pre-flooding period, the two PCs contributed to 75.32 % of the total variance in the dataset. During pre-flooding season, PC 1 and PC 2 explained 47.37 % and 27.95 % of the total variance, respectively (Table 4). Major contributors to PC 1 include pH, BOD, Fe, Pb, Cu, Cl, Na and K, which indicate a combined influence of domestic discharge, urban runoff, atmospheric deposition and geogenic influence during the dry season, when dilution is minimal. The dilution factor mainly depends on the river and the area of the catchment [33]. PC 2 has strong positive loadings on pH, EC, COD, Ca, Mg, SO_4, HCO_3^-, TH, TDS, Mn and Zn, which suggests anthropogenic sources and geogenic input through mineral dissolution and bedrock interaction. During post-flooding period, PC 1 and PC 2 explained 46.53% and 26.21% of the total variance, respectively (Table 4). The dominant parameter on PC 1 include EC, DO, BOD, COD, TH, Mg, Fe, K, Cl, Ca, and Ni, suggesting land surface runoff, agricultural leaching and dissolution of mineral-containing rocks. pH, TDS, Na, SO_4, HCO_3, Cu, Zn and Mn dominated PC 2, which may be attributed to contributions from leaching, erosion and also geogenic input. The results from PCA show that anthropogenic and geogenic sources play an important role in determining the water quality of the Jia Bharali River.

Table 4. Loadings of water quality parameters in Jia Bharali River

Parameter	Pre-flood components		Post-flood components	
	PC 1	**PC 2**	**PC 1**	**PC 2**
pH	0.706	-0.026	0.102	0.815
EC	0.309	0.702	-0.744	0.028
DO	0.764	0.286	0.732	0.016
TH	-0.619	0.682	-0.749	0.502
TDS	0.452	0.769	0.452	- 0.864
COD	0.348	0.825	0.698	0.245
BOD	0.926	-0.504	0.616	-0.321
Na	0.829	0.319	0.250	0.909
K	0.818	0.547	0.915	0.247
Ca	0.441	-0.617	0.674	-0.094
Mg	0.662	-0.886	0.818	-0.186
HCO_3	0.538	-0.616	0.232	-0.846
Cl	-0.785	0.456	0.905	-0.207
SO_4	0.085	0.740	-0.445	0.663
Fe	0.822	0.394	0.781	0.262
Cu	0.818	-0.275	0.098	0.605
Zn	0.482	0.621	0.522	0.756

Parameter	Pre-flood components		Post-flood components	
	PC 1	PC 2	PC 1	PC 2
Mn	-0.401	0.833	-0.327	0.723
Pb	0.708	0.268	0.394	-0.409
Ni	-	-	0.603	0.527
Cd	0.673	0.464	-	-
Eigenvalues	2.640	1.017	2.413	1.031
% variance	47.37	27.95	46.53	26.21

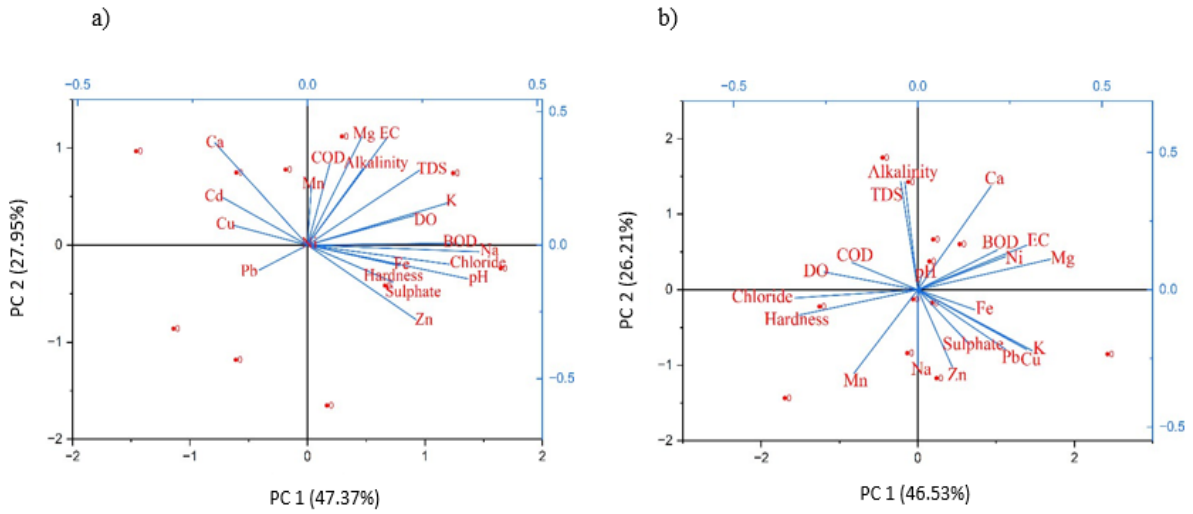

Figure 5. PCA biplot of water quality parameters of Jia Bharali River during a) pre-flood, and b) post-flood periods 2024

4. Conclusions

The present study of hydrogeochemical and spatiotemporal evaluation of the Jia Bharali River in response to flooding provides crucial insights into the river's water quality during two seasons, pre-flood and post-flood. The findings indicate that most of the water quality parameters are within the permissible limits of WHO (2017) and BIS (2012), although certain elements such as Fe, Mn, and Zn exhibited a relative increase during the pre-flooding season, likely due to low water levels and anthropogenic inputs. The seasonal trend also shows dilution effects during post-flooding period, confirming the impact of hydrological variability on the river water chemistry. The total hardness of the water samples was high during both seasons; however, the pre-flood season showed relatively higher concentration than the post-flood period. Ca^{2+} -Mg^{2+} - HCO_3^- type is the major hydrochemical facies of the water samples of the Jia Bharali River. Gibbs plot diagram suggests that rock weathering process primarily controls the water chemistry of the river. PCA identified pollution sources and underlying factors influencing water quality. HCA grouped data points into three and five similar clusters of water quality parameters based on sampling sites for pre-flood and post-flood periods, respectively. The pollution indices (HPI, HEI, C_d, and PLI) confirmed a low pollution status of the Jia Bharali River. However, proper monitoring of the river is essential to mitigate risks associated with heavy metals in the future, by taking into consideration the flood events along the Jia Bharali River. This study establishes an important baseline for Jia Bharali River and

underscores the need for regular monitoring to ensure sustainable utilisation of freshwater resources amid growing developmental pressures.

Multidisciplinary Domains

This research covers the domains: a) Hydrochemistry, b) Environmental Monitoring, and c) Environmental Chemistry.

Funding

This research was funded by the DST (Department of Science & Technology) Core Research Grant (CRG/2022/000538) received by Sumi Handique and the UGC (University Grant Commission) NET-JRF (Reference No. 210510604028) received by Jigyashree Lahon.

Acknowledgment

The authors are highly grateful to the Sophisticated Analytical Instrumentation Centre of Tezpur University for providing access to carry out some of the analysis.

Conflicts of Interest

The authors declare no conflict of interest.

Declaration on AI Usage

The authors declare that the article has been prepared without the use of AI tools.

References

[1] Wang, H.; He, G. Rivers: linking nature, life, and civilization. *River,* **2022***, 1*(1): 25–36. https://doi.org/10.1002/rvr2.7

[2] Sharma, R.; Kumar, R.; Satapathy, S.C.; Al-Ansari, N.; Singh, K.K.; Mahapatra, R.P.; et al. Analysis of water pollution using different physicochemical parameters: A study of Yamuna River. *Frontiers in Environmental Science,* **2020**, *8*, 581591. https://doi.org/10.3389/fenvs.2020.581591

[3] Dixit, S.; Tiwari, S. Impact assessment of heavy metal pollution of Shahpura Lake, Bhopal, India. *International Journal of Environmental Research,* **2007***, 2(1)*: 37-42.

[4] Krishnakumar, A.; Jose, J.; Kaliraj, S.; Aditya, S.K.; Krishnan, K.A. Assessment of the impact of flood on groundwater hydrochemistry and its suitability for drinking and irrigation in the River Periyar Lower Basin, India. *Environmental Science and Pollution Research,* **2022**, *29*(19), 28267-28306. https://doi.org/10.1007/s11356-021-17596-y

[5] Saeed, T.U.; Haleema Attaullah, H. A. Impact of extreme floods on groundwater quality (in Pakistan). *British Journal of Environment and Climate Change,* **2014**, 4(1), 133151. https://doi.org/10.9734/BJECC/2014/4105

[6] Wang, Z.; Li, X.; Hou, X. Hydrogeochemistry of river water in the upper reaches of the datong river basin, china: Implications of anthropogenic inputs and chemical weathering. *Acta Geologica Sinica-English Edition,* **2021**, *95*(3), 962-975. https://doi.org/10.1111/1755-6724.14525

[7] Richards, L.A.; Fox, B.G.; Bowes, M.J.; Khamis, K.; Kumar, A.; Kumari, R.; et al. A systematic approach to understand hydrogeochemical dynamics in large river systems: Development and application to the River Ganges (Ganga) in India. *Water research,* **2022**, 211, 118054. https://doi.org/10.1016/j.watres.2022.118054

[8] Saha, A.; Saikia, K.K.; Handique, S. Distribution characteristics of microplastics and potentially toxic elements as co-contaminants in groundwater in mid-Brahmaputra Valley, northeastern India. *Environmental Monitoring and Assessment,* **2025**, *197*(7), 121. https://doi.org/10.1007/s10661-025-14266-1

[9] Debnath, J.; Sahariah, D.; Saikia, A.; Meraj, G.; Nath, N.; Lahon, D.; et al. Shifting sands: assessing bankline shift using an automated approach in the Jia Bharali River, India. *Land,* **2023**, *12*(3), 703. https://doi.org/10.3390/land12030703

[10] Debnath, J.; Sahariah, D.; Nath, N.; Saikia, A.; Lahon, D.; Islam, M. N.; et al. Modelling on assessment of flood risk susceptibility at the Jia Bharali River basin in Eastern Himalayas by integrating multicollinearity tests and geospatial techniques. *Modeling earth systems and environment*, **2024,** *10*(2), 2393-2419. https://doi.org/10.1007/s40808-023-01912-1

[11] Khound, N. J.; Bhattacharyya, K.G. Assessment of water quality in and around Jia-Bharali River basin, North Brahmaputra Plain, India, using multivariate statistical technique. *Applied Water Science,* **2018**, *8*, 1-21. https://doi.org/10.1007/s13201-018-0870-z

[12] Ramachandran, A.; Krishnamurthy, R.R.; Jayaprakash, M.; Shanmugasundharam, A. Environmental impact assessment of surface water and groundwater quality due to flood hazard in Adyar River Bank. *Acta Ecologica Sinica,* **2019**, *39*(2), 125-132. https://doi.org/10.1016/j.chnaes.2018.08.008

[13] Lim, K. Y.; Zakaria, N.A.; Foo, K.Y. Geochemistry pollution status and ecotoxicological risk assessment of heavy metals in the Pahang River sediment after the high magnitude of flood event. *Hydrology Research,* **2021**, *52*(1), 107-124. https://doi.org/10.2166/nh.2020.122

[14] Lahon, J.; Handique, S. Flood-induced variation and source apportionment of microplastics in Jia Bharali River of mid-Brahmaputra Valley, India. *Environmental Monitoring and Assessment,* **2024**, *196*(12), 1236. https://doi.org/10.1007/s10661-024-13432-1

[15] Khound, N.J.; Phukon, P.; Bhattacharyya, K.G. Physico-chemical studies on surface water quality in the Jia-Bharali River basin, North Brahmaputra plain, India. *Archives of applied science research,* **2012**, *4(2),* 1169-1174.

[16] Pollution Control Board, Assam. Action plan for Jia Bharali River near NH-15 crossing, **2019.**Available online:https://pcbassam.org/RRC%20Action%20Plan%20Final/priority%20V/Jia%20Bharali%20River.pdf (accessed on 25th August, 2025).

[17] Wang, L.; Wang, Y.; Xu, C.; An, Z.; Wang, S. Analysis and evaluation of the source of heavy metals in water of the River Changjiang. *Environmental monitoring and assessment,* **2011**, *173*(1), 301-313. https://doi.org/10.1007/s10661-010-1388-5

[18] Dutta, S.; Dwivedi, A.; Suresh Kumar, M. Use of water quality index and multivariate statistical techniques for the assessment of spatial variations in water quality of a small river. *Environmental monitoring and assessment,* **2018**, *190*(12), 718. https://doi.org/10.1007/s10661-018-7100-x

[19] American Public Health Association. Standard methods for the examination of water and wastewater (20th ed.), **1995.** Available online: http://www.standardmethods.org/ (accessed on 5 August **2025**).

[20] Sheykhi, V.; Moore, F. Geochemical characterization of Kor River water quality, fars province, Southwest Iran. *Water quality, exposure and health,* **2012***, 4*, 25-38. https://doi.org/10.1007/s12403-012-0063-1

[21] Chiamsathit, C.; Auttamana, S.; Thammarakcharoen, S. Heavy metal pollution index for assessment of seasonal groundwater supply quality in hillside area, Kalasin, Thailand. *Applied Water Science,* **2020**, *10(6)*, 1-8. https://doi.org/10.1007/s13201-020-01230-2

[22] Mohan, S.V.; Nithila, P.; Reddy, S.J. Estimation of heavy metals in drinking water and development of heavy metal pollution index. *Journal of Environmental Science & Health Part A,* **1996**, *31(2)*, 283-289. https://doi.org/10.1080/10934529609376357

[23] Rajkumar, H.; Naik, P.K.; Rishi, M.S. A new indexing approach for evaluating heavy metal contamination in groundwater. *Chemosphere,* **2020**, *245*, 125598.https://doi.org/10.1016/j.chemosphere.2019.125598

[24] Esshaimi, M.; Ouazzani, N.; Avila, M.; Perez, G.; Valiente, M.; Mandi, L. Heavy metal contamination of soils and water resources Kettara abandoned mine. *American Journal of Environmental Sciences,* **2012**, Vol. 8, No. 3, 253-261. https://doi.org/10.5555/20123268632

[25] Varol, M. Assessment of heavy metal contamination in sediments of the Tigris River (Turkey) using pollution indices and multivariate statistical techniques. *Journal of Hazardous Materials,* **2012,** *195*, 355-364. https://doi.org/10.1016/j.jhazmat.2011.08.051

[26] Bureau of Indian Standards (BIS). Indian standard (10500: 2012) Drinking Water- Specification (Second Revision) 2012. Available online: https://www.bis.gov.in/other/DrinWatIS10500.pdf (accessed on 24 July **2025**).

[27] Mohan, I.; Jasrotia, R.; Dhar, S.; Bhau, B.S.; Pathania, D; Khargotra, R. Pollution indices and correlation of heavy metals contamination in the groundwater around brick kilns in Jammu and Kashmir, India. *Heliyon*, **2024,** 10(6). https://doi.org/10.1016/j.heliyon.2024.e27869

[28] Gautam, S.K.; Tripathi, J.K.; Singh, S.K. Assessing the suitability of Ghaghra River water for irrigation purpose in India. In Agricultural Water Management **2021**; pp. 67- 81. Academic Press. https://doi.org/10.1016/B978-0-12-812362-1.00005-9

[29] Kumar, P.; Singh, A.N.; Shrivastava, R.; Mohan, D. Assessment of seasonal variation in water quality dynamics in river Varuna-a major tributary of River Ganga. *International Journal of Advanced Research,* **2015**, *3(3),* 1176-1193.

[30] Jithesh, M.; Radhakrishnan, M.V. Seasonal variation in water quality parameters of Chaliyar river, Kerala, southern India. *Environment and Ecology,* **2020**, *38 (1*): 71—77.

[31] World Health Organization (WHO). Guidelines for drinking-water quality (4th edition). World Health Organization, Geneva 2017. Available online: 7.https://www.who.int/publications/i/item/9789241549950 (accessed on 28 July **2025**).

[32] Environment (Protection) Rules (Schedule VI) 1986. Ministry of Environment, Forest and Climate Change, Government of India. Available online:https://moef.gov.in/uploads/2018/03/THE_ENVIRONMENT.pdf (accessed on 4 August **2025**).

[33] Khan, M.Y.A.; Gani, K.M.; Chakrapani, G.J. Spatial and temporal variations of physicochemical and heavy metal pollution in Ramganga River—a tributary of River Ganges, India. *Environmental Earth Sciences,* **2017**, *76*, 1-13. https://doi.org/10.1007/s12665-017-6547-3

[34] Gupta, D.; Kaushik, S.; Shukla, R.; Mishra, V.K. Mechanisms controlling major ion chemistry and its suitability for irrigation of Narmada River, India. *Water Supply,* **2022**, *22(3*), 3224-3241. https://doi.org/10.2166/ws.2021.408

[35] Naik, P.K.; Awasthi, A.K.; Anand, A.V.S.S.; Behera, P.N. Hydrogeochemistry of the Koyna river basin, India. *Environmental Earth Sciences,* **2009**, *59*(3), 613-629. https://doi.org/10.1007/s12665-009-0059-8

[36] Sharma, G.; Lata, R.; Thakur, N.; Bajala, V.; Kuniyal, J.C.; Kumar, K. Application of multivariate statistical analysis and water quality index for quality characterization of Parbati River, Northwestern Himalaya, India. *Discover Water,* **2021**, *1*, 1-20. https://doi.org/10.1007/s43832-021-00005-3

[37] Benmerabet, N.; Sedrati, N.; Djabri, L. Hydrogeochemical processes, water–rock interactions, and the suitability of groundwater in a semi-arid region, Northeastern Algeria. *Water Supply,* **2025**, *25*(3), 404-423. https://doi.org/10.2166/ws.2025.023

[38] Raj, V.T.; Gayathri, J.A.; Vandana, M.; Sreelash, K.; Maya, K.; Sajan, K. Rock–water interaction, chemical weathering and solute transport of two rivers draining contrasting climate gradients in Western Ghats, India. *Earth Surface Processes and Landforms,* **2023**, *48*(10), 1969-1989. https://doi.org/10.1002/esp.5598

[39] da Costa, I.D. Costa, L.L.; Zalmon, I.R. Micro plastics in water from the confluence of tropical rivers: Overall review and a case study in Paraiba do Sul River basin. *Chemosphere,* **2023**, *338*, 139493. https://doi.org/10.1016/j.chemosphere.2023. 139493

Appendix

Table S1. Sampling locations of the Jia Bharali River with their coordinates and elevations

Sample sites	Latitude	Longitude	Elevation (metres)
S1	27.0007	92.431	164
S2	26.5951	92.431	164
S3	26.0007	92.4607	163
S4	26.5726	92.492	126
S5	26.5526	92.505	92
S6	26.5056	92.5146	86
S7	26.4916	92.5229	84
S8	26.4617	92.5207	86
S9	26.4538	92.5237	86
S10	26.4426	92.5059	86
S11	26.4145	92.5133	87
S12	26.3915	92.5141	85

Table S2. Heavy metal concentration at each sampling location of Jia Bharali River during pre-flooding period of 2024

Sample site	Fe (mg/L)	Cu (mg/L)	Mn (mg/L)	Zn (mg/L)	Pb (mg/L)	Cd (mg/L)
1	0.003 ± 0.367	0.0008 ± 0.072	0.0983 ± 0.759	0.1703 ± 0.052	0.0019 ± 1.03	-
2	-	0.0006 ± 0.1248	0.0061 ± 0.964	0.1352 ±0107	0.00173 ± 0.929	0.00019 ± 0.09
3	-	0.0008 ± 0.955	0.0003 ± 0.0145	0.1249 ± 0.022	0.00118 ± 0.130	-
4	-	0.0008 ± 0.0778	0.0029 ± 0.1491	0.2159 ± 0.064	-	0.00003 ± 0.19
5	0.0126 ± 0.858	0.0005 ± 0.475	0.0006 ± 0.0872	0.6132 ± 0.104	0.00045 ± 0.541	-
6	0.0063 ± 0.0338	0.0002 ± 0.0572	0.0002 ± 0.0095	0.4754 ± 0.187	-	-
7	0.0002 ± 0.1438	0.0005 ± 0.0952	-	0.5252 ± 0.122	0.00143 ± 0.868	-
8	0.001 ± 0.2583	0.0003 ± 0.1108	-	0.3655 ± 0.335	0.00202 ± 1.225	-
9	0.0015 ± 0.1008	0.0006 ± 0.0852	0.0002 ± 0.0058	0.0551 ± 0.1568	0.0005 ± 1.4362	-
10	0.0022 ± 0.3233	0.0005 ± 0.0784	0.0257 ± 0.174	0.0735 ± 0.0249	0.00067 ± 0.438	-
11	0.0014 ± 0.359	0.0007 ± 0.0438	0.0018 ± 0.2113	0.3494 ± 0.080	0.00077 ± 0.771	-
12	0.0034 ± 3.393	0.001 ± 0.0839	0.0004 ± 0.0254	0.1921 ± 0.121	-	-
Max	0.01260	0.00100	0.09830	0.61320	0.00202	0.00019
Min	0.00020	0.00020	0.00020	0.05510	0.00045	0.00003
Range	0.01240	0.00080	0.09810	0.55810	0.00157	0.00016

Table S3. Heavy metal concentration at each sampling location of Jia Bharali River during post-flooding period of 2024

Sample site	Fe (mg/L)	Cu (mg/L)	Mn (mg/L)	Zn (mg/L)	Pb (mg/L)	Ni (mg/L)
1	0.0052 ± 0.0003	0.0002 ±0.00001	0.0035 ± 0.00003	0.0759 ±0.0003	-	-
2	0.0383 ± 0.0011	0.0002 ± 0.000002	0.0129 ± 0.0001	0.0231 ±0.0001	-	-
3	0.0208 ± 0.0011	0.0004 ± 0.000005	0.00324 ± 0.00005	0.0433 ±0.0003	0.0002±0.01	-
4	0.0195 ± 0.006	0.0002 ± 0.000020	0.00130 ± 0.00001	0.0121 ±0.0002	-	-
5	0.0128 ± 0.0006	0.0003 ± 0.000002	0.0006 ± 0.000001	0.0021 ±0.002	-	-
6	0.0063 ± 0.0004	0.0003 ± 0.00007	0.00022 ±0.000001	0.0016 ± 0.0002	-	0.0001 ± 0.001
7	0.1233 ± 0.0004	0.0005 ± 0.000013	0.00497 ± 0.00002	0.001 ± 0.0001	0.0001±0.02	0.0001 ± 0.002
8	0.0575 ± 0.0007	0.0002 ± 0.000004	0.0021 ±0.000003	0.0254 ± 0.0001	-	-
9	0.0232 ± 0.0004	0.0001 ± 0.000002	0.00089 ±0.00001	0.0234 ± 0.0002	-	-
10	0.0037 ± 0.0006	0.0001 ± 0.000002	0.00019 ±0.0004	0.0004 ± 0.0003	-	-
11	0.031 ± 0.0002	0.004 ± 0.0002	0.0031 ± 0.0001	0.022 ± 0.00031	0.0001±0.01	-
12	0.056 ± 0.0006	0.0052 ± 0.0005	0.0032 ± 0.0003	0.082 ± 0.00013	0.00017±0.1	0.00012 ±0.003
Max	0.1233	0.0052	0.01291	0.082	0.0002	0.00012
Min	0.0037	0.0001	0.000193	0.0004	0.0001	0.0001
Range	0.1196	0.0051	0.012717	0.0816	0.0001	0.00002

Table S4. Rainfall data of the study area for the two sampling periods (16th -30th April and 1st -15th September, 2024) [A1]

Data &Time	Data Value (mm)
2024-04-16T08:30:00	0.600000024
2024-04-16T17:30:00	0
2024-04-17T08:30:00	25
2024-04-17T17:30:00	0
2024-04-18T08:30:00	0
2024-04-18T17:30:00	0
2024-04-19T08:30:00	1.600000024
2024-04-19T17:30:00	0
2024-04-20T08:30:00	4.800000191
2024-04-20T17:30:00	0
2024-04-21T08:30:00	16.20000076
2024-04-21T17:30:00	0
2024-04-22T08:30:00	0
2024-04-22T17:30:00	0
2024-04-23T08:30:00	0
2024-04-23T17:30:00	0
2024-04-24T08:30:00	0
2024-04-24T17:30:00	0
2024-04-25T08:30:00	0
2024-04-25T17:30:00	0
2024-04-26T08:30:00	0
2024-04-26T17:30:00	0
2024-04-27T08:30:00	23

Data &Time	Data Value (mm)
2024-04-27T17:30:00	0
2024-04-28T08:30:00	1.600000024
2024-04-28T17:30:00	0
2024-04-29T08:30:00	17
2024-04-29T17:30:00	0
2024-04-30T08:30:00	0
2024-04-30T17:30:00	0
2024-09-01T02:30:00	0
2024-09-01T05:30:00	0
2024-09-01T08:30:00	0.200000003
2024-09-01T11:30:00	0
2024-09-01T14:30:00	0
2024-09-01T17:30:00	0
2024-09-01T20:30:00	0
2024-09-01T23:30:00	0
2024-09-02T02:30:00	0
2024-09-02T05:30:00	0
2024-09-02T08:30:00	0
2024-09-02T11:30:00	0
2024-09-02T14:30:00	0
2024-09-02T17:30:00	0
2024-09-02T20:30:00	0
2024-09-02T23:30:00	0
2024-09-03T02:30:00	0
2024-09-03T05:30:00	0
2024-09-03T08:30:00	0
2024-09-03T11:30:00	0
2024-09-03T14:30:00	0
2024-09-03T17:30:00	0
2024-09-03T20:30:00	0
2024-09-03T23:30:00	0
2024-09-04T02:30:00	0
2024-09-04T05:30:00	0
2024-09-04T08:30:00	0
2024-09-04T11:30:00	0
2024-09-04T14:30:00	0
2024-09-04T17:30:00	0
2024-09-04T20:30:00	0
2024-09-04T23:30:00	0
2024-09-05T02:30:00	0
2024-09-05T05:30:00	0
2024-09-05T08:30:00	19
2024-09-05T11:30:00	0
2024-09-05T14:30:00	0
2024-09-05T17:30:00	0

Data &Time	Data Value (mm)
2024-09-05T20:30:00	0
2024-09-05T23:30:00	0
2024-09-06T02:30:00	0
2024-09-06T05:30:00	0
2024-09-06T08:30:00	0
2024-09-06T11:30:00	0
2024-09-06T14:30:00	0
2024-09-06T17:30:00	0
2024-09-06T20:30:00	0
2024-09-06T23:30:00	0
2024-09-07T02:30:00	0
2024-09-07T05:30:00	0
2024-09-07T08:30:00	0
2024-09-07T11:30:00	0
2024-09-07T14:30:00	0
2024-09-07T17:30:00	0
2024-09-07T20:30:00	0
2024-09-07T23:30:00	0
2024-09-08T02:30:00	0
2024-09-08T05:30:00	0
2024-09-08T08:30:00	0
2024-09-08T11:30:00	0
2024-09-08T14:30:00	0
2024-09-08T17:30:00	0
2024-09-08T20:30:00	0
2024-09-08T23:30:00	0
2024-09-09T02:30:00	0
2024-09-09T05:30:00	0
2024-09-09T08:30:00	0
2024-09-09T11:30:00	0
2024-09-09T14:30:00	0
2024-09-09T17:30:00	0
2024-09-09T20:30:00	0
2024-09-09T23:30:00	0
2024-09-10T02:30:00	0
2024-09-10T05:30:00	0
2024-09-10T08:30:00	11.60000038
2024-09-10T11:30:00	0
2024-09-10T14:30:00	0
2024-09-10T17:30:00	0
2024-09-10T20:30:00	0
2024-09-10T23:30:00	0
2024-09-11T02:30:00	0
2024-09-11T05:30:00	0
2024-09-11T08:30:00	3

Data &Time	Data Value (mm)
2024-09-11T11:30:00	0
2024-09-11T14:30:00	0
2024-09-11T17:30:00	0
2024-09-11T20:30:00	0
2024-09-11T23:30:00	0
2024-09-12T02:30:00	0
2024-09-12T05:30:00	0
2024-09-12T08:30:00	18
2024-09-12T11:30:00	0
2024-09-12T14:30:00	0
2024-09-12T17:30:00	0
2024-09-12T20:30:00	0
2024-09-12T23:30:00	0
2024-09-13T02:30:00	0
2024-09-13T05:30:00	0
2024-09-13T08:30:00	0
2024-09-13T11:30:00	0
2024-09-13T14:30:00	0
2024-09-13T17:30:00	0
2024-09-13T20:30:00	0
2024-09-13T23:30:00	0
2024-09-14T02:30:00	0
2024-09-14T05:30:00	0
2024-09-14T08:30:00	0
2024-09-14T11:30:00	0
2024-09-14T14:30:00	0
2024-09-14T17:30:00	0
2024-09-14T20:30:00	0
2024-09-14T23:30:00	0
2024-09-15T02:30:00	0
2024-09-15T05:30:00	0
2024-09-15T08:30:00	0
2024-09-15T11:30:00	0
2024-09-15T14:30:00	0
2024-09-15T17:30:00	0
2024-09-15T20:30:00	0
2024-09-15T23:30:00	0

[A1] India-WRIS (National Water Informatics Centre). Rainfall data for Tezpur. Available online: https://indiawris.gov.in/wris/#/timeseriesdata (accessed on 30 March **2026**).